

Experimental Results on Tungsten-Wire Explosions in Air at Atmospheric Pressure—Comparison with a One-Dimensional Numerical Model¹

A. Kloss,² A. D. Rakhel,³ and H. Hess^{2, 4}

Experimental results on exploding tungsten wires in air at atmospheric pressure at current densities $\geq 10^7 \text{ A} \cdot \text{cm}^{-2}$ and a current rise $\geq 10^{10} \text{ A} \cdot \text{s}^{-1}$ are presented. Besides the current through the probe and the voltage across it, the diameter of the wire material and its surface temperature have been measured. The final aim of this investigation is the determination of the thermophysical properties of a high-melting liquid metal up to its critical point. Here a first step should be made to demonstrate the reliability of the method and to justify the crucial assumptions. To determine the limits for the applicability of a homogeneous approach used so far, a one-dimensional numerical model in Z-pinch geometry has been used which gives the time evolution of the profiles of temperature, density, and pressure across the wire. The model describes well the main features observed in these experiments. A physical explanation for the maximum in the time dependences of the surface temperature is proposed. This behavior is related to special thermodynamic properties of a two-phase (liquid-gas) mixture forming in a peripheral layer around the liquid metal. The temperature limit is determined for which there are no remarkable gradients of temperature and density across the wire. The specific heat, the thermal expansion coefficient, and the electrical as well as thermal conductivity of liquid tungsten can now, in principle, be obtained. The parameters of the critical point of the liquid-vapor phase transition can also be estimated.

KEY WORDS: critical point; electrical conductivity; evaporation; exploding wires; high temperatures; refractory metals; thermal expansion; tungsten.

¹ Paper presented at the Thirteenth Symposium on Thermophysical Properties, June 22–27, 1997, Boulder, Colorado, U.S.A.

² Institute of Low-Temperature Plasma Physics, University of Greifswald, Robert-Blum-Str. 8-10, D-17489 Greifswald, Germany.

³ Incorporated Institute of High Temperatures, High Energy Density Research Centre, Izhorskaya 13/19, Moscow 127412, Russia.

⁴ To whom correspondence should be addressed.

1. INTRODUCTION

To study thermophysical properties of fluids of refractory metals up to critical-point conditions, i.e., at the high values of critical temperatures, it is necessary to generate the corresponding material states by pulse heating methods. As a first approximation, the density and temperature of the expanding material can be determined from the measured expansion radius and surface temperature, assuming a homogeneous density and temperature distribution over the cross section and a constant emissivity in the liquid. The pressure, however, has to be calculated using an adequate equation of state.

Using fast electrical discharges through wire-shaped probes of the studied material—so-called wire explosions—near-critical point conditions for tungsten have been reached. A discussion of the results has shown some discrepancies which could not be solved in the framework of a homogeneous model. For “slow” explosions an assumed vaporization plateau similar to the well-known melting plateau had been found [1]. The corresponding energy, however, was always too small to vaporize the entire material. Regardless of a strong increase in the energy input rate, the temperature reaches a maximum between 12,000 and 14,000 K, while the energy is monotonically increasing.

These observations can be explained only in the case of a radial dependence of the quantities characterizing the material state. A model has been used to describe the heating and subsequent expansion of the wire material which takes into account its electrodynamic, hydrodynamic, thermodynamic, and transport properties and an approximate equation of state for the fluid state including the liquid–gas phase transition.

2. EXPERIMENTAL ARRANGEMENT

Critical values for the liquid–gas phase transition of high-melting metals lie in a range around 10,000 K and 1 GPa [2]. Whereas lower values can be attained in high-pressure cells, such conditions can be reached only during fast wire explosions. If these explosions are carried out in an environment at atmospheric pressure, a very high rate of energy dissipation is necessary to reach high pressures in the material. This requires a steep increase in the current and a sufficient adaptation of the circuit impedance to that of the wire.

The fundamental design of the experiment is described in detail in Ref. 1. A coaxial capacitor is surrounded by a copper tube. It is discharged through a spark gap into a wire which consists of the studied material

(tungsten). The entire circuit without the wire has a capacitance of 345 nF and an inductance of 57 nH.

The current is measured simultaneously in two ways: first, by means of a coaxial shunt resistor and, second, by numerical integration of the signal of a Rogowski coil. Both methods agree within 3%. The numerically integrated signal was used for further evaluations because of its better signal-to-noise ratio. The voltage is measured with a low-inductance ohmic divider. This signal also contains an inductive part which is proportional to the derivative of the current. More than 90% of this inductive part is compensated by a small coil that is connected antiparallel to the voltage divider. The remaining part is then numerically corrected in a way that the cold resistance of the sample is fitted best. The current and voltage are measured with a precision of 0.5%. The current signals of different experiments with all parameters kept constant scatter less than 2%. The voltage signal scatter is about 3%. The dissipated energy e and the resistance R are calculated from the so determined current I and the ohmic voltage.

The diameter of the expanding wire is taken from a streak image in a spectral range from 550 to 850 nm showing the time development of the luminous heated wire. For each instant of time, the distance between the maximum derivatives of brightness is determined and taken for the diameter. This method is reasonable due to observed radial profiles with a flat top and steep edges that give proof of a homogeneous surface temperature according to Lambert's law. From the start-up to the end of melting, the self-luminosity is small; therefore, the results from Ref. 3 are used here. Shadowgraphs are not useful, because the wire is surrounded by a thin insulating layer to avoid surface discharges. The optical influence of this layer is corrected. The radii are measured with a precision of 3% and a scatter of 7%.

The surface temperature of the sample is determined from the radiation at 650 nm. A spot (15- μ m diameter) is displayed on the entrance of a fiber which is connected with a Si-PIN diode. In the diode signal the melting plateau is identified and used for self-calibration of the pyrometer. Assuming the emissivity to be constant above the melting temperature, a surface temperature was calculated from the radiation signal using Planck's law. Due to its shape the level of the melting plateau was determined with an error of about 10%. This causes an uncertainty in the temperature of less than 8%.

The entire wire is observed during the explosion with a fast framing camera. Four images, with an exposure time of 10 ns each, ensure that no parallel discharges and no change of length of the wire occur during the observation time. In addition, the homogeneity of the sample and the reliability of the temperature and radius determinations are analyzed.

Important for passing the critical region during a wire explosion is the selection of an appropriate specimen. Its resistance has to match the impedance of the discharge circuit, and its mass has to be evaporated during the first half period of the discharge. Its radius has to be smaller than the skin depth, and special care has to be taken to prevent parallel surface discharges. The circuit used here has a natural frequency of about 1.2 MHz and an impedance of about 0.3Ω . The skin depth for tungsten is then about $110 \mu\text{m}$, so that in a stationary case, a wire with a radius of $37.5 \mu\text{m}$ is not affected. The dynamic skin effect leads to a relaxation time of approximately 10 ns and therefore has to be considered only before melting. With a length of 5.0 mm the cold resistance of $83 \text{ m}\Omega$ (measured) matches well, and the mass could be evaporated twice with the maximum supplied energy.

The time for balancing out small pressure differences should be small compared with the experimental time scale. Using a sound speed of $4 \text{ km} \cdot \text{s}^{-1}$ the time for crossing the radius is about 10 ns.

Clean tungsten wires show strong surface discharges at surface temperatures above 6000 K. An oxidized surface diminishes this effect due to the higher work function of tungsten oxide. Best results were obtained with wires coated with polytetrafluorethylene (PTFE). The fluorine accepts the thermally emitted electrons in such an amount that the observation times can be extended beyond the time of passing through the critical region. Thus, tungsten wires (length of 5.0 mm, diameter of $75 \mu\text{m}$) with a transparent coating of $20\text{-}\mu\text{m}$ PTFE [4] were used.

3. THEORY

To describe the motion of material and distributions of electric and magnetic fields during the pulse heating process, a one-dimensional magnetohydrodynamic model in Z-pinch geometry [5, 6] is used. In this geometry, the velocity of the material has only a radial component u , the electrical current density has only a component along the axis j , and the magnetic field strength has only an azimuthal component H . For this case the laws of conservation of mass, momentum, and energy can be written as

$$\frac{\partial \rho}{\partial t} + \frac{1}{r} \frac{\partial}{\partial r} (r \rho u) = 0 \quad (1)$$

$$\frac{\partial u}{\partial t} + u \frac{\partial u}{\partial r} = -\frac{1}{\rho} \frac{\partial p}{\partial r} - \frac{jH}{c\rho} \quad (2)$$

$$\frac{\partial s}{\partial t} + u \frac{\partial s}{\partial r} = \frac{jE'}{\rho T} \quad (3)$$

where ρ , p , T , and s are the density, pressure, temperature, and specific entropy, respectively. All the variables are functions of the radius vector r and the time t . The electric field strength E' in the reference frame which is at rest in relation to the material particles can be calculated from the Lorentz formula, $E' = E + uH/c$, where E is the electrical field strength in the laboratory frame of reference, and c is the speed of light in vacuum; here and below in this section all equations of the theoretical model are presented in the cgs (Gaussian) system.

The boundary conditions for the system of Eqs. (1)–(3) were derived in Ref. 7. The task about the evaporation of a metal from the surface of a sample heated by a high-density electrical current pulse ($j \sim 10^7 \text{ A} \cdot \text{cm}^{-2}$) was solved. The following expressions give the pressure and the temperature on the sample surface:

$$p(a, t) = 0.56P_s(T(a, t)) \quad (4)$$

$$T(a, t) = T_b - \frac{B}{j} \exp\{-\lambda_0/[RT(a, t)]\} \quad (5)$$

where $a = a(t)$ is the radius of the sample, $P_s(T)$ is the saturated vapor pressure, R is the molar gas constant, and λ_0 is the molar heat of evaporation at $T = 0 \text{ K}$. $T_b = T(a - \delta, t)$ is the bulk temperature being defined as the temperature at the distance δ from the surface; $a \gg \delta \geq \sqrt{\chi t}$ (χ is the thermal diffusivity). B is practically a constant when $T < 0.9T_c$ (T_c is the critical temperature for the liquid–gas phase transition). The parameter B can be expressed through some thermodynamic parameters of liquid metal near its normal melting point (for more details, see Ref. 7, pp. 1014–1018).

The system of equations for the total current in a RCL circuit containing the wire can be written as

$$\frac{L_0 + L}{c^2} \frac{dI}{dt} + \frac{I}{2c^2} \frac{dL}{dt} + E(a, t)l + U_c = 0 \quad (6)$$

$$\frac{dU_c}{dt} = I/C_0 \quad (7)$$

where L_0 and L are the inductance of the circuit and the wire, respectively, $U_c(t)$ is the capacitor bank voltage, and C_0 is the capacitance.

The initial conditions for the task are as follows: $p = 0.1 \text{ MPa}$, $T = 300 \text{ K}$, $U_c(0) = U_0$, and $I(0) = 0$. To make the set of equations complete, we need the equation of state, i.e., the dependences $p(\rho, T)$ and $s(\rho, T)$, and the electrical conductivity $\sigma(\rho, T)$.

The equation of state used for the calculations was a so-called soft-sphere equation [8], which was further modified in Ref. 9: an additional fitting parameter was introduced to describe the data on expanded liquid transition metals. The main reasons for using this equation of state were its simple form and its successful application to expanded metals [2].

The free energy for this equation of state can be presented by

$$F = F_0(\rho) + F_i(\rho, T) + F_r(\rho, T) \quad (8)$$

where F_0 is the so-called cold part, F_i is the ideal-gas contribution, and F_r is an additional repulsive contribution.

$$F_0 = \frac{R\Theta}{\mu} (C_n x^{n/3} - x^m) \quad (9)$$

$$F_i = -\frac{R\Theta}{\mu} y [\ln(y^{3/2}/x) + \text{const}] \quad (10)$$

$$F_r = \frac{R\Theta}{\mu} \frac{Q(n+4)}{2} x^{n/9} y^{2/3} \quad (11)$$

Here the variables $x = \rho/w$ and $y = T/\Theta$ are used. μ is the molar weight and C_n is the fcc Madelung constant for the pair power potential (the so-called repulsive soft-sphere potential) with the power index n . The equation of state contains five fitting parameters: w , Θ , m , n , and Q . The parameters were chosen to reproduce the experimental values of some thermodynamic parameters of liquid tungsten: the densities near the melting and boiling points at atmospheric pressure, the heat of evaporation at the boiling temperature, and also the thermal expansion coefficient, the sound velocity, and the isobaric specific heat. To satisfy all of these conditions for tungsten, it was necessary to introduce one additional fitting parameter in this equation of state: instead of the fixed ideal-gas specific heat 3/2 (the power index of y in the ideal-gas term), a fitting parameter was used.

The electrical conductivity over a wide area of the phase diagram of tungsten (solid, liquid, plasma, and gas) was obtained on the basis of theoretical models and comparisons with an experimental data set [10].

The Godunov method was used to solve the hydrodynamic part of the system of equations, Eqs. (1)–(3) [11]. Maxwell's equations for Z-pinch geometry [6] together with Eqs. (6)–(9) were solved by the tridiagonal inversion method [12].

4. DISCUSSION

In Fig. 1 the temporal dependencies of the experimental electrical data and the corresponding curves given by the model can be seen; the agreement is remarkable. Figure 2 shows the time dependence of the pyrometrically measured surface temperature of the sample and the calculated temperatures for different radial layers of the sample. The layers divide the sample into 41 concentric circles or zones, containing a fixed mass of the material between them. These 40 layers present a set of Lagrangian's coordinates used in our calculations. The upper curve (axis) in Fig. 1 corresponds to the layer surrounding 10% of the total mass; the lower curve (surface) corresponds to those surrounding 90% of the mass. The other three curves correspond to 30, 50, and 70% of the mass, respectively. For the experimental curve as well as for curves representing the outer layers, a temperature maximum is observed. It should be noted that the energy input continues to increase even after the maximum occurs (see Fig. 1). This behavior of the temperature of the outer layers is caused by a rapid expansion of the two-phase mixture appearing in these layers. Therefore, this temperature maximum indicates that the boiling curve has been reached by at least a part of the material (this was intuitively assumed

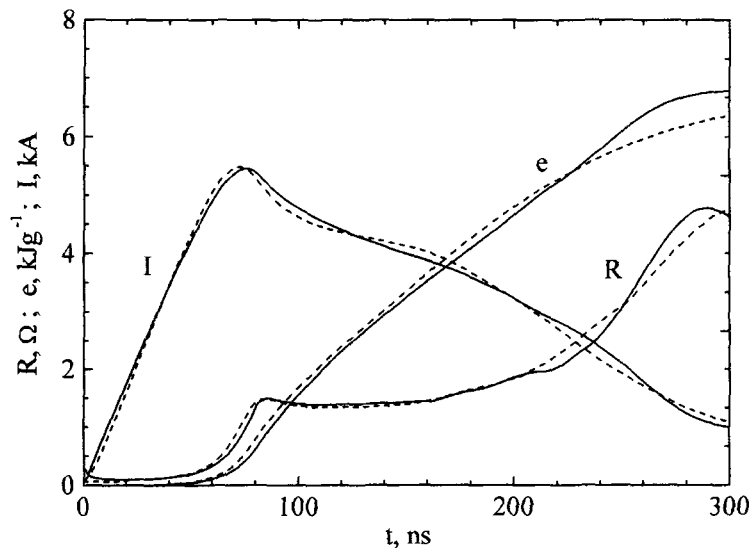


Fig. 1. Electrical data of a wire explosion (current I , dissipated energy e , and resistance R): the solid lines show the experimental values for an initial capacitor voltage of $U_c(0) = 4.6$ kV; the dashed lines show corresponding model calculations.

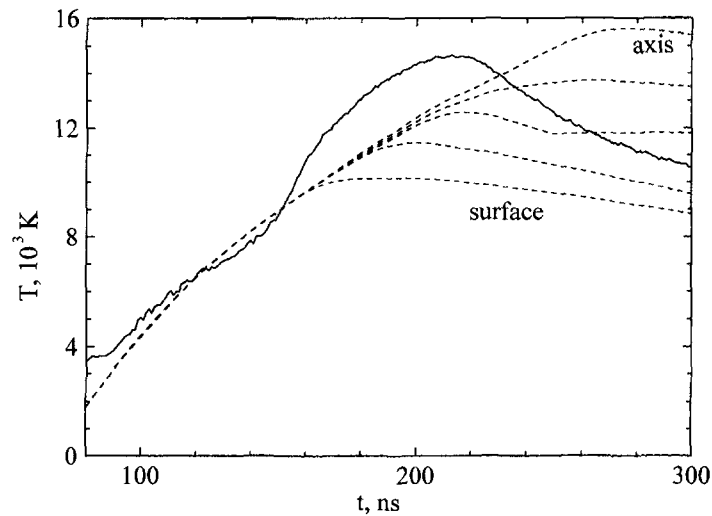


Fig. 2. Temperature versus time for a wire explosion as in Fig. 1. The solid line gives the pyrometrically measured surface temperature of the sample. The dashed lines show temperatures of consecutive layers from the model calculations.

earlier [13]). The stronger increase in the experimentally determined temperature at $T > 8000$ K could be disguised by an increase in the emissivity due to the generation of bubbles in a small layer on the surface. As one can see, a homogeneous distribution of the temperature across the area of the sample can be assumed up to a surface temperature $T \leq 10,000$ K.

In Fig. 3, the V - T diagram is presented. In the model the inner part of the material passes the critical density above the critical temperature as a one-phase fluid. The outer part passes below the critical temperature forming a two-phase layer. Due to the extremely low sound speed in this layer (for more details, see Ref. 7), the core may reach the required pressure.

The experimentally determined temperature which characterizes a layer near the surface should be corrected for temperatures above 8000 K due to an expected increasing emissivity. Its maximum should not exceed the critical temperature.

It seems to be possible to describe the main features of the studied wire explosion with the model presented here. This gives confidence in future applications to the complex processes during the fast heating of refractory metals up to critical parameters.

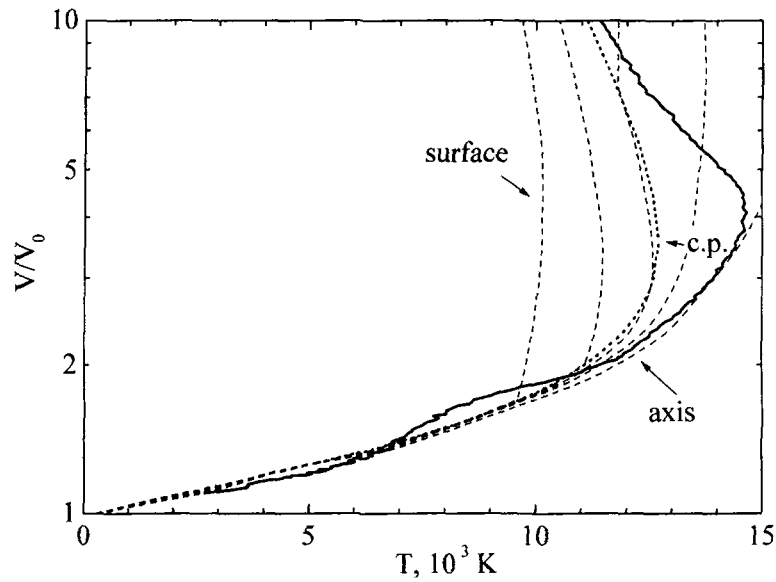


Fig. 3. Volume versus temperature for a wire explosion as in Fig. 1; V_0 is the initial volume of the solid. The solid line gives the experiment. The dashed lines are from model calculations; the different radial layers are indicated. The dotted curve is the boundary of the coexistence region; the critical point (c.p.) is shown.

REFERENCES

1. A. Kloss, T. Motzke, R. Grossjohann, and H. Hess, *Phys. Rev. E* **54**:5851 (1996).
2. G. R. Gathers, *Rep. Prog. Phys.* **49**:341 (1986).
3. R. S. Hixson and M. A. Winkler, *Int. J. Thermophys.* **11**:709 (1990).
4. Goodfellow GmbH Catalog (1996/1997), p. 261.
5. A. V. Bushman, V. S. Vorob'ev, A. D. Rakhel, and V. E. Fortov, *Sov. Phys. Dokl.* **35**:1079 (1990).
6. A. V. Bushman, V. S. Vorob'ev, V. N. Korobenko, A. D. Rakhel, A. I. Savvatimskii, and V. E. Fortov, *Int. J. Thermophys.* **14**:565 (1993).
7. A. D. Rakhel, *Int. J. Thermophys.* **17**:1011 (1996).
8. W. G. Hoover, G. Stell, E. Goldmark, and G. D. Degani, *J. Chem. Phys.* **63**:5434 (1975).
9. D. A. Young, UCRL-52352 (Lawrence Livermore Laboratory, 1977).
10. V. S. Vorob'ev and A. D. Rakhel, *Teplofiz. Vys. Temp.* **28**:18 (1990).
11. S. K. Godunov, A. V. Zabrodin, M. Ya. Ivanov, A. N. Kraiko, and G. A. Prokopov, *Numerical Solution of Many-Dimensional Gas Dynamic Tasks* (Nauka, Moscow, 1976).
12. A. A. Samarski and Yu. P. Popov, *Difference Methods for Solution of Gas Dynamic Tasks* (Nauka, Moscow, 1980).
13. H. Hess, E. Kaschnitz, and G. Pottlacher, *High Press. Res.* **12**:29 (1994).